Annals of Glaciology 14 1990

THE IMPACT OF MILANKOVITCH SOLAR RADIATION VARIATIONS ON SEA-ICE AND AIR TEMPERATURE IN A COUPLED ENERGY-BALANCE CLIMATE–SEA-ICE MODEL

by

Tamara Shapiro Ledley

(Department of Space Physics and Astronomy and the Earth Systems Institute, Rice University, P.O. Box 1892, Houston, TX 77251, U.S.A.)

ABSTRACT

The sensitivity of thermodynamically-varying sea-ice and surface air temperature to variations in solar radiation on the 10^4 to 10^5 time scales is examined in this study. Model simulation results show the mean annual sea-ice thickness is very sensitive to the magnitude of mid-summer solar radiation. During periods of high mid-summer solar radiation between 115 ka B.P. and the present the sea ice is thinner, producing larger summer time leads and longer periods of open ocean. This has an effect on the mean annual sea-ice thickness, but not on the mean annual air temperature. However, the changes in sea ice are accompanied by similar variations in the summer surface air temperature, which are the result of the variations in the solar radiation and meridional energy transport.

INTRODUCTION

The physical mechanisms that cause the 100 ka glacial/interglacial cycle found in the geologic record are not well understood. One potentially important factor in producing these cycles is sea ice, and the impact it has in controlling moisture and energy exchanges between the ocean and the atmosphere. In this study, the response of thermodynamically-varying sea-ice and surface air temperatures to changes in short wave radiation at the top of the atmosphere, on the 10^4 to 10^5 year time scales, is examined through the use of a coupled energy-balance climate – thermodynamic sea-ice model (the CCSI model).

CCSI MODEL

The CCSI model treats four distinct regions of the climate system, each of which is represented by a single layer (Fig. 1). These regions are the air over land, the air over ocean, a mixed layer ocean, and a ground layer. The version of the model used in this study computes 336 time steps per year and employs a 10° latitudinal grid, with land–sea resolution in each zone distributed in accordance with current land–sea distribution.

The CCSI model predicts the future air layer temperatures through the use of a simple explicit finite differencing scheme. The energy fluxes that are included in this calculation are the horizontal heat transports, meridional and zonal; short and long wave radiative fluxes; sensible heat flux; and latent heat flux. The horizontal energy fluxes between land and sea within a zone and between latitude zones are computed using a diffusion parameterization similar to that used by North and Coakley (1979) and Ledley (1988), and the horizontal fluxes between zones in the ocean are specified. The vertical energy fluxes are computed at the top of the atmosphere over ocean and land (and for short wave radiation, over sea ice), and at the surface over ocean, sea ice, and land. The model simulates seasonal cycles, a necessary feature for studying the impact of sea-ice variations on climate.

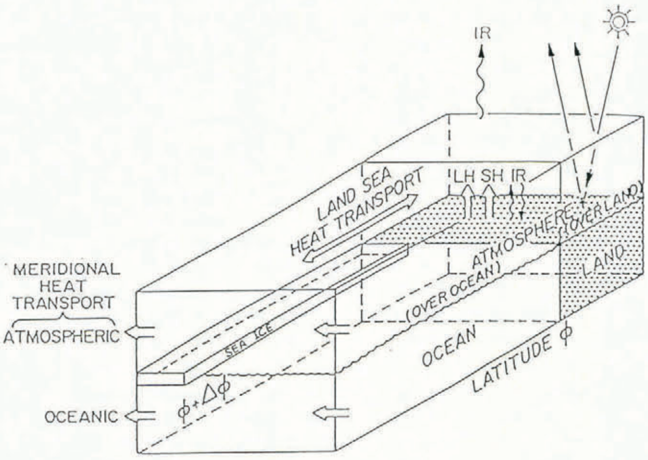

Fig. 1. Schematic diagram of coupled energy-balance climate — thermodynamic sea-ice model. LH = latent heat flux; ☼ = solar radiation; SH = sensible heat flux; Φ = latitude; IR = infrared radiation.

The thermodynamic sea-ice model that is used in the CCSI model is that described by Ledley (1985a and b) and is based on the models of Semtner (1976) and Maykut and Untersteiner (1971). It is a three-layer thermodynamic model that includes conduction within the ice, penetration of solar radiation into the ice layers, and surface energy balances.

The CCSI model does not explicitly compute the dynamic processes involved in lead formation. Therefore, the formation of new sea ice on open ocean, and the opening and closing of leads are computed following the techniques of Ledley (1987). In this parameterization a minimum lead fraction (MLF, representing the minimum fraction of open ocean within the ice pack that is formed due to dynamic processes during the winter) of the total ice/ocean area to be occupied by leads during the winter, is specified.

A parameterized transport of sea ice into equatorward latitude zones is included in the model. The sea-ice transport parameterization has four main parameters. These control when ice can be transported, the response of the ocean temperature to the transported ice, and also include the MLF, and the fraction of the ice displaced by the opening of leads that is ridged or transported. This parameterized transport is described in more detail in Ledley (1990, this volume).

A detailed description of the CCSI model is given in Ledley (1988).

THE EXPERIMENTS

Originally six experiments were conducted with the CCSI model in which the solar radiation was varied to

https://doi.org/10.3189/S0260305500008454 Published online by Cambridge University Press

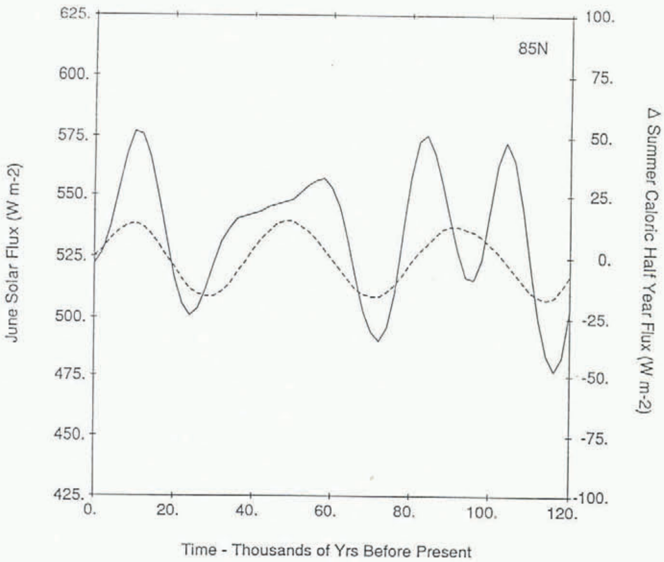

Fig. 2. June solar radiation at the top of the atmosphere (solid line), and the change in the summer caloric half-year solar radiation from present (dashed line) over the past 120 000 years, in $W\ m^{-2}$ at 85°N. Similar variations occur at 75° and 65°N.

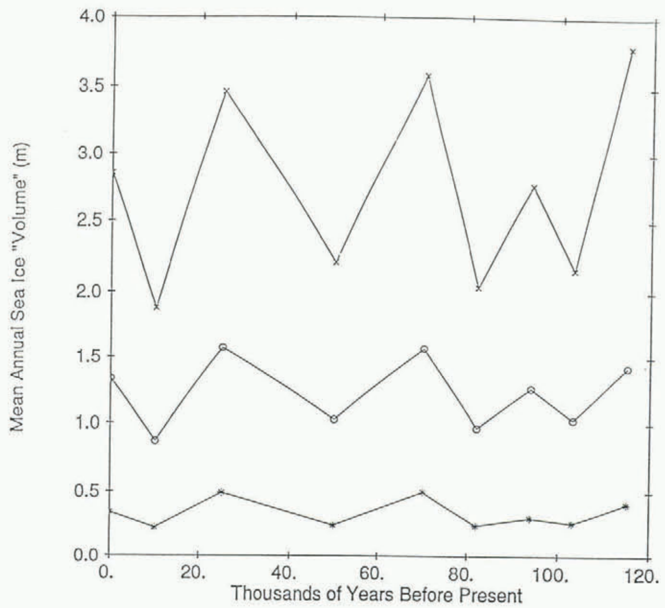

Fig. 3. Mean annual sea-ice "volume" at 85°N (×), 75°N (o), and 65°N (*) for nine solar radiation regimes during the past 115 ka. The sea-ice "volume", defined as the average of the sea-ice thickness times one minus the lead fraction, is expressed in m of ice.

correspond to times of extreme summer caloric half-year insolation over the past 115 000 years (Fig. 2). The times that correspond to periods of relatively high summer caloric half-year insolation in the Northern Hemisphere are 10 000, 50 000, and 94 000 years B.P. and the times that correspond to periods of relatively low summer caloric half-year insolation in the Northern Hemisphere are 25 000, 70 000, and 115 000 years B.P. (hereafter referred to as # ka B.P.). These times were selected as the maxima and minima in the caloric summer half-year radiation at the North Pole from Figure 2 of Ruddiman and McIntyre (1981) and from Vernekar (1972).

In order to determine the importance of the summer caloric half-year solar radiation compared to the maximum solar radiation during the summer on the sea-ice variations and climate, two additional experiments were performed. These were at 82 ka and 103 ka B.P. At these times the solar radiation at the solstice was at a relative maximum (see Fig. 2).

The model was run for 20 model years which takes 35 s on the Cray XMP/48 at the National Center for Atmospheric Research. This brought the simulations to equilibrium in all of the experiments. In the case of 115 ka B.P. the equilibrium was a repeating 2-year cycle; however, the differences between these two years were very small. Therefore, in the figures the model results for 115 ka B.P. year 20 are plotted.

EFFECT OF MILANKOVITCH SOLAR RADIATION VARIATIONS ON SEA-ICE THICKNESS AND CONCENTRATION

The impact of the changes in the solar radiation on the mean annual sea-ice "volume", where the sea-ice "volume" is defined as the sea-ice thickness times the fraction of the ocean area in the zone that is covered by sea ice, is shown in Figure 3. In most cases the times with relatively low mean annual sea-ice "volume" correspond to times with a high summer caloric half-year solar radiation, as shown in Figure 2. However, at 82 ka and 103 ka the mean annual sea-ice "volume" shows a significant decrease from present, while the summer half-year solar radiation at the top of the atmosphere is relatively unchanged from present.

The immediate cause of this anomaly in the response of the sea-ice "volume" to the summer caloric half-year solar radiation at 82 ka and 103 ka B.P. is the relative maximum in the maximum summer solar radiation at the top of the atmosphere at those times. At 82 ka and 103 ka B.P. the maximum summer solar radiation is high compared to that at 94 ka. The short-term seasonal maximum in solar radiation occurs during the relatively short melt season of sea ice, on the order of one month, resulting in thinner ice at 82 ka and 103 ka B.P. as compared to 94 ka B.P. The high summer maximum in solar radiation at 82 ka and 103 ka B.P. is not reflected in the summer caloric half-year radiation because at those times the solar radiation rises and drops quickly in the spring and fall respectively compared to at 94 ka B.P. This seasonal variation in solar radiation causes the summer caloric half-year solar radiation at 82 ka and 103 ka to be similar to that at present and lower than at 94 ka B.P.

Therefore, the important factor in controlling sea-ice thickness is the maximum summer solar radiation. This is reflected in the variations of the mean annual sea-ice "volume" (Fig. 3), which follow the variations of the maximum summer solar radiation (Fig. 2).

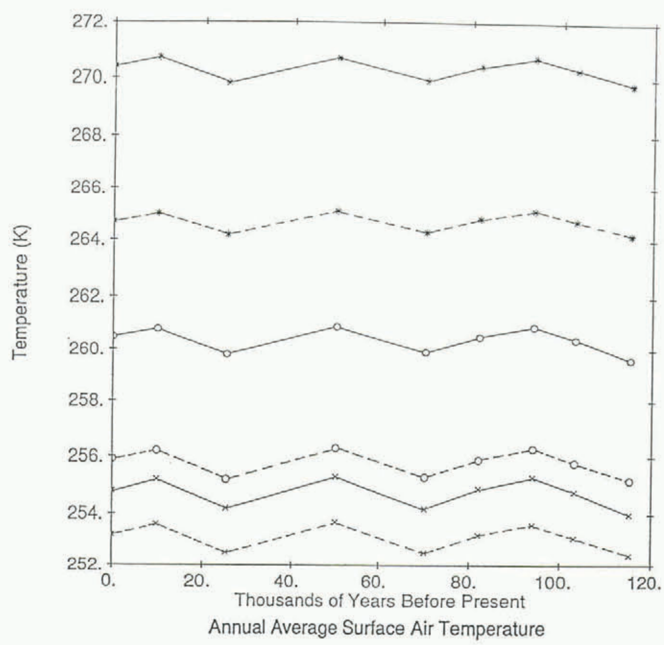

Fig. 4. Annual average surface air temperature over ocean and sea ice (solid lines) and over land (dashed lines) at 85°N (×), 75°N (o), and 65°N (*) over the past 115 ka.

https://doi.org/10.3189/S0260305500008454 Published online by Cambridge University Press

EFFECT OF MILANKOVITCH SOLAR RADIATION VARIATIONS ON SURFACE AIR TEMPERATURES

Variations in the maximum summer insolation have a small direct impact on the mean annual surface air temperature because the maximum occurs for only a small fraction of the year; therefore, the shorter-term variations in sea ice at 82 ka and 103 ka B.P. do not appear in the mean annual surface air temperature (Fig. 4). However, the changes in sea-ice thickness and concentration produced by the variations in the maximum solar radiation are accompanied by similar changes in the maximum summer surface air temperature over land and over ocean (Fig. 5).

The main cause of variations in summer surface air temperature as simulated in this study is the variation in the absorbed short wave radiation in the climate system. This is produced by changes in the incoming summer solar radiation at the top of the atmosphere, which directly affects surface air temperature over land, ocean, and sea ice; and in sea-ice albedo resulting from the changes in sea-ice concentration.

An additional effect is the impact that changes in the incoming summer solar radiation have on the meridional energy convergence in the air over the ocean and sea ice. Since the land has a much lower thermal inertia than the ocean, the surface air temperatures over land are much more sensitive to the change in the solar radiation at the top of the atmosphere. This has a dramatic effect on the meridional surface air temperature gradient between land and ocean in adjacent latitude zones, affecting the meridional energy convergence, and thus enhancing the direct effect of the solar radiation variations on the surface air temperature over ocean and sea ice.

DISCUSSION

An interesting feature of the surface air temperatures shown in Figure 5 is that the differences between the summer surface air temperature over land and ocean within a zone is smaller at 75°N than at 85°N and 65°N. This is partially a result of the land–sea distribution in those latitude zones. There is a very large land–ocean boundary between 65°N and 75°N (land to the south). During the summer the large air temperature gradient from ocean to land in those zones leads to a large meridional energy transport from air over land to air over ocean (from 65°N to 75°N). This produces a warming of the air over the ocean at 75°N to a greater degree than at either 85°N or 65°N, which have smaller ocean–land boundaries with adjacent zones. Air temperature gradients from ocean to land are largest in the middle of the summer and probably reverse during the winter. As a result the annual average surface air temperatures are distinctly different over land and ocean within each latitude zone.

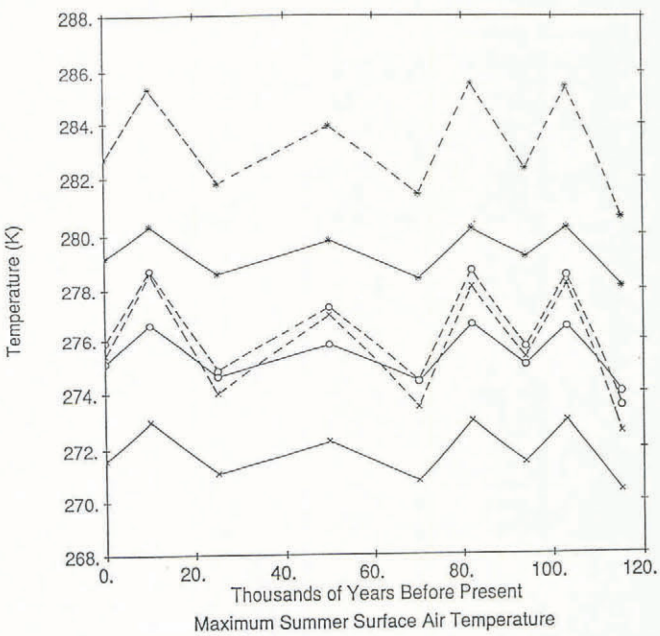

Fig. 5. Maximum summer surface air temperature over ocean and sea ice (solid lines) and over land (dashed lines) at 85°N (×), 75°N (o), and 65°N (*) over the past 115 ka.

Figure 5 also indicates that at 115 ka B.P. the surface air temperatures were colder than at present; however, the geologic record indicates that the Earth was in the midst of an interglacial, similar to today. The reason for this discrepancy is that in this study only the impact of the solar radiation variations on the sea ice and its effect on surface air temperatures are examined. Changes over land surfaces, such as ice sheets, are not considered; and the effect of the hydrologic cycle, especially with respect to moisture fluxes and snowfall over both land and ocean, not considered. While at 115 ka B.P. the Earth was in the midst of an interglacial, the solar radiation regime was changing toward lower values of short wave radiation, possibly triggering the beginning of the last ice age. However, all of the feedbacks that would contribute to this change in climate, especially land ice and the hydrologic cycle, are not yet included in the CCSI model.

SUMMARY

In summary, simulations of the climate at 0, 10, 25, 50, 70, 82, 94, 103, and 115 ka B.P. with a coupled energy-balance climate—thermodynamic sea-ice model show that the mean annual sea-ice thickness and the summer surface air temperatures vary with changes in maximum summer solar radiation. The maximum solar radiation affects the sea-ice thickness through its impact on the sea ice during its short melt season, and its subsequent impact on the summertime leads and periods of open ocean. Maximum solar radiation affects summer surface air temperature both directly, and through the impact of changes in the sea-ice concentration on surface albedo, and thus on the short wave radiation absorbed in the climate system. During other periods of the year the changes in the sea-ice concentration are not as dramatic as during the summer, and the incoming solar radiation in the polar regions is very low; therefore, the shorter term variations between 70 ka and 115 ka B.P. seen in the mean sea-ice thickness and the summer surface air temperatures do not appear in the annual average surface air temperatures.

The direct effect of the solar radiation on surface air temperatures over both land and ocean also has a large impact on the meridional energy convergence in each zone. This is because of the lower thermal inertia of land as compared to ocean. During periods of higher summer solar radiation the air over the land warms more than the air over the ocean. This produces a large meridional temperature gradient, and thus an increase in meridional energy convergence, which enhances the effect of the increases in solar radiation in the air over the ocean.

ACKNOWLEDGEMENTS

This work was supported in part by grants from the Climate Dynamics section of the National Science Foundation, ATM-8706587 and ATM-8904437. This material is also based in part upon work supported by the Texas Advanced Technology Program under grant 3639.

REFERENCES

Ledley, T.S. 1985a. Sea ice: multiyear cycles and white ice. *J. Geophys. Res.*, **90**(D3), 5676-5686.

Ledley, T.S. 1985b. Sensitivity of a thermodynamic sea ice model with leads to time step size. *J. Geophys. Res.*, **90**(D1), 2251-2260.

Ledley, T.S. 1987. Development of a new sea ice growth and lead parameterization. *Climate Dynamics*, 2(2), 91-100.

Ledley, T.S. 1988. A coupled energy balance climate-sea ice model: impact of sea ice and leads on climate. *J. Geophys. Res.*, **93**(D12), 15,919-15,932.

Ledley, T.S. 1990. Meridional sea ice transport and its impact on climate. *Ann. Glaciol.*, **14**, 141-143.

Maykut, G.A. and N. Untersteiner. 1971. Some results from a time-dependent thermodynamic model of sea ice. *J. Geophys. Res.*, **76**(6), 1550-1575.

North, G.R. and J.A. Coakley, *jr.* 1979. Differences between seasonal and mean annual energy balance model calculations of climate and climate sensitivity. *J. Atmos. Sci.*, **36**, 1189-1204.

Ruddiman, W.F. and A. McIntyre. 1981. Oceanic mechanisms for amplification of the 23,000-year ice-volume cycle. *Science*, **212**(4495), 617-627.

Semtner, A.J., *jr.* 1976. A model for the thermodynamic growth of sea ice in numerical investigations of climate. *J. Phys. Oceanogr.*, **6**(3), 379-389.

Vernekar, A.D. 1972. Long-period global variations of incoming solar radiation. *Meteorol. Monogr.* 12.